THE GEOLOGICAL SOCIETY OF AMERICA®

Eastern Ghats Province (India)–Rayner Complex (Antarctica) accretion: Timing the event

Pritam Nasipuri[1], F. Corfu[2], and A. Bhattacharya[3]
[1]DEPARTMENT OF EARTH AND ENVIRONMENTAL SCIENCES AND CREST, INDIAN INSTITUTE OF SCIENCE EDUCATION AND RESEARCH, BHOPAL, INDIA
[2]DEPARTMENT OF GEOSCIENCES AND CEED, UNIVERSITY OF OSLO, OSLO, NORWAY
[3]DEPARTMENT OF GEOLOGY AND GEOPHYSICS, INDIAN INSTITUTE OF TECHNOLOGY, KHARAGPUR 721 302, INDIA

ABSTRACT

There is consensus that, at 1.0–0.9 Ga, the granulites in the Eastern Ghats Province (EGP), Eastern India, and the Rayner Complex, Antarctica, were parts of a coherently evolved crustal block. Paleogeographic reconstructions suggest that in the Neoproterozoic/Early Paleozoic, India and Antarctica were closely positioned at equatorial latitudes in two periods at 1.0–0.9 Ga and 0.6–0.5 Ga. The question is, in which of these periods did the EGP–India vis-à-vis India–Antarctica accretion occur. Top-to-the-west thrusts juxtaposed the EGP with the Bastar Craton, a part of the Greater India landmass. The eastern fringe of the craton underwent anatexis (750–780 °C; 8–9 kbar) and high deformation strain that demonstrably weakened westward. Zircon in the anatectic migmatites at the EGP margin and in the weakly-deformed and non-migmatite granite in the hinterland in the west yields U–Pb upper intercept ages of 2.5–2.4 Ga whereas titanite, hosted in the leucosome of a metatexite and in a granite, has an age of 502 ± 3 Ma coinciding with the lower intercept ages of zircon discordia lines. The lack of 1.0–0.9 Ga dates in the cratonic margin suggests that the EGP accreted with the Bastar Craton and the Greater India landmass at 0.5 Ga during the Gondwanaland assembly, and not in the Early Neoproterozoic. It is within the realms of possibility that the EGP had already separated from the Rayner Complex during the disintegration of Rodinia, and therefore, the 0.5 Ga accretion of the dismembered EGP with Greater India may not be symptomatic of India–Antarctica accretion, in spite of the proximity of the two landmasses inferred from paleogeographic reconstructions.

LITHOSPHERE; v. 10; no. 4; p. 523–529; GSA Data Repository Item 2018166 | Published online 18 April 2018 https://doi.org/10.1130/L703.1

INTRODUCTION

Paleogeographic reconstructions (Fig. 1A) suggest that India and Antarctica were closely positioned at equatorial latitudes in the Early Neoproterozoic (1.0–0.9 Ga) and in the Late Neoproterozoic/Early Paleozoic, 0.6 and 0.5 Ga (Torsvik, 2003; Li et al., 2008). In the intervening period, broadly overlapping with the dispersal of crustal fragments of the Rodinia supercontinent, the Greater India landmass was positioned at northern latitudes, whereas the Australo-Antarctic Block was broadly stationary near the equator (Torsvik, 2003; Li et al., 2008; Fig. 1A). Several researchers (Black et al., 1987; Dalziel, 1997; Mezger and Cosca, 1999; Halpin et al., 2005; Morrissey et al., 2015) argue that the metamorphic histories of the granulites in the Eastern Ghats Province, India (EGP) and in the Rayner Complex (Antarctica) are similar, and the two crustal domains probably constituted a coherently evolved landmass by 1.0–0.9 Ga (Fig. 1B). This leads to the question whether the Greater India landmass and Antarctica (inclusive of the EGP) were juxtaposed in the Early Neoproterozoic (Dalziel, 1997; Black et al., 1987; Mezger and Cosca, 1999; Chattopadhyay et al., 2015), or whether the accretion occurred in the Late Neoproterozoic/Early Cambrian (Biswal et al., 2007) or Middle/Late Cambrian coinciding with the final phase of Gondwanaland assembly (Bhattacharya et al., 2016; Chatterjee et al., 2017). We address this vexed issue based on field observations, petrological studies, and U–Pb zircon and titanite geochronology using Isotope Dilution Thermal Ionization Mass Spectrometry (ID-TIMS) of granitoids and anatectic migmatites in the cratonic granites and gneisses. The results are crucial for delineating the assembly of crustal fragments in the East Gondwanaland.

GEOLOGICAL BACKGROUND

Early Paleoproterozoic/Neoarchean granitoids (Fig. 1C; Data Repository File DR1[1] for geochemical data) of the Bastar Craton (Mohanty, 2015, and references there in) are juxtaposed with the ensemble of Early Neoproterozoic high-T granulites, massif anorthosite and syenite plutons, and expansive megacrystic orthopyroxene-bearing granitoids of the EGP along its northwestern and northern margins (Rickers et al., 2001). At Ranmal, Orissa, the cratonic granites (quartz, K-feldspar, plagioclase, biotite, hornblende, ilmenite, titanite ± epidote, with apatite and zircon as accessory minerals) experienced polyphase anatexis (Figs. 1D–1F) in response to top-to-the-west thrusting of the EGP over the Bastar Craton (Bhadra et al., 2007).

[1]GSA Data Repository Item 2018166, File DR1: Whole rock major element oxides (in wt %), trace and rare earth element oxides (in ppm) of Ranmal migmatite complex; File DR2: Back-scatter electron images of textural relations in Ranmal migmatites; File DR3: Electron probe microanalysis data, structural formulae of minerals (A) and (B) P-T conditions in Ranmal migmatite complex; File DR4: Photomicrographs of representative zircon grains selected for analyses; File DR5: Plot of zirconium concentrations in anatectic and foliated granites from Ranmal (whole rock data, this study and Bhadra et al., 2007), is available at http://www.geosociety.org/datarepository/2018, or on request from editing@geosociety.org.

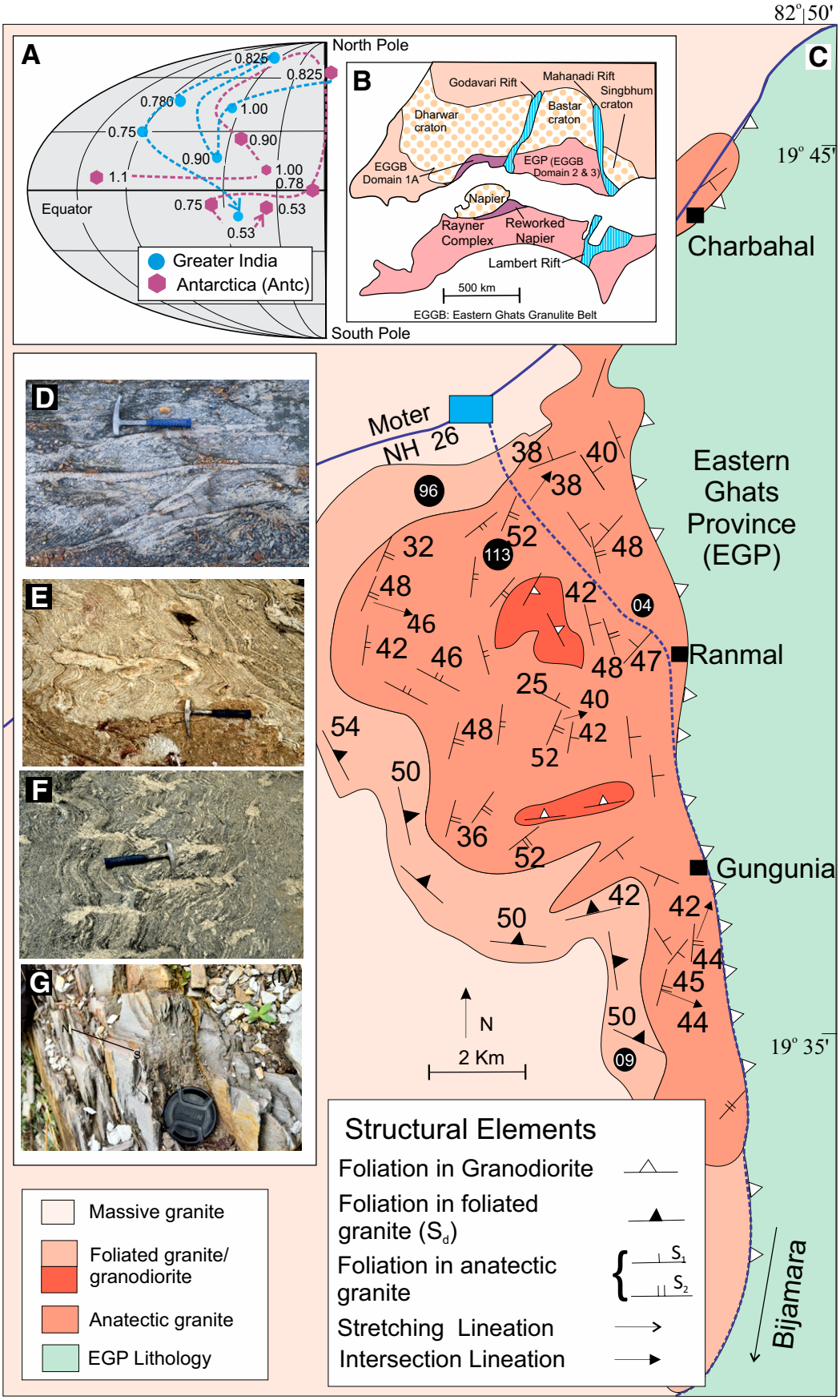

Figure 1. (A) Paleogeographic positions of India and Antarctica in the period between 1.1 and 0.5 Ga (adopted from Li et al., 2008). Dots correspond to centrally located points in India and Antarctica, and the keyed ages are from Li et al. (2008). (B) Reconstruction of 1.0–0.9 Ga Eastern Ghats Province (EGP)–Rayner Complex assembly across the facing coast lines of India and Antarctica (after Veevers and Saeed, 2009). (C) Geological map of the Ranmal migmatite complex in the Bastar Craton at the margin of the EGP. Filled circles are sample locations with sample numbers. (D–G) Field relations in Bastar polyphase anatectic migmatites adjacent to EGP neighboring Ranmal. (D) Isoclinal to tight F_2 folds on S_1 metatexite layers in migmatite, and S_1 leucosomes curving into N-trending S_2 melt-filled shears (hammer head points north). (E, F) Open F_2 folds on S_1 metatexite layers with development of diatexite melt pods along axial planes of F_2 folds. Note the F_2 folds are tighter close to the diatexite melt pods, and the metatexite leucosomes are continuous with the S_2 diatexites. The features imply that progressive deformation and melt production were synchronous. (G) N-trending subvertical foliation (marked by dash line) in intensely tectonized phyllites along the eastern fringe of the Mesoproterozoic Chattisgarh basin sediments unconformably overlying the 2.5–2.4 Ga deformed granite (not in image) in the cratonic hinterland (lens cap for scale).

In the anatectic granites of the craton, stromatic biotite-rimmed leucosome layers (S_1) in alternations with biotite-hornblende defined mesosomes (File DR2A, DR2B) are folded into asymmetric west-vergent tight/isoclinal folds (F_2; Figs. 1D–1F) with variable plunges. The axial planes of F_2 folds are filled by leucosome layers that form networks of N-trending channels that coalesce to form coarse-grained diatexite melt pods (Figs. 1D–1F). The axial planar leucosomes (S_2) are continuous with the folded S_1 leucosome layers (Figs. 1E–1F). The S_1 stromatic layers are folded near the S_2 diatexite segregations, but the folds die out progressively distal from the diatexite melt pods (Figs. 1E–1F).

In the leucosomes, trains of tiled plagioclase grains, and rational faces of euhedral feldspars impinging into neighboring quartz films attest to syn-deformational melt emplacement. In the metatexite mesosomes, the dominance of dispersed weakly-strained/unstrained grains with high-energy boundaries, weak alignment among subhedral feldspar crystals subparallel to shape-preferred biotite (X_{Mg} = 0.35, TiO_2 ~ 4.4 wt%, File DR3A) aggregates, plumose margins of quartz grains, and quartz films against subhedral feldspar boundaries (File DR2C) attest to deformation of the anatexites at high-temperature. The features imply that the polyphase anatexis in the craton was broadly contemporaneous with progressive deformation/thrusting EGP over the Bastar Craton. Hornblende- (X_{Mg} = 0.31 − 0.32, File DR3A) plagioclase (X_{Ca} = 0.19 − 0.20, File DR3A) thermometry (Holland and Blundy, 1994) and hornblende-plagioclase-quartz barometry (Bhadra and Bhattacharya, 2007) in the S_1 mesosomes indicate that melting in the migmatites occurred at ~750–780 °C and 8–9 kbar (File DR3B).

Westwards and progressively more distal from the EGP–Bastar Craton interface the granitoids in the cratonic footwall vary from mylonitic in the east, through foliated and then to massive (lacking mesoscopic fabrics) varieties in the hinterland. The critical minerals in deformed and anatectic granites defining the thrust fabric vary from biotite-amphibole in the east (this study) through epidote-amphibole to chlorite-epidote in the weakly-deformed granites in the west (Bhadra et al., 2007). In these zones, the eastern margins of the Khariar basin (basin initiation at 1.455 ± 0.047 Ga; Das et al., 2009) and the Chattisgarh basin (basin initiation at ca. 1 Ga; Das et al., 2009) unconformably overlying the Bastar granites are sheared along the eastern margin (Fig. 1G), but are undeformed farther west (Chakraborty et al., 2015). This testifies to the westward decrease in the strain intensity as a consequence of the EGP–BC accretion.

U–Pb GEOCHRONOLOGY

ID-TIMS U–Pb analyses in zircon and titanite in the Bastar granitoids were carried out in anatectic migmatites located within 200 m (sample 04) and ~2 km (sample 113) from the Bastar Craton–EGP contact, non-anatectic foliated granite (sample 9 and 96) located around 2 and ~4 km west of the thrust contact (Fig. 1C).

Zircon was separated by crushing, and subsequently separated by Wilfley table, heavy liquid and magnetic procedures. Zircon grains were hand-picked and subjected to chemical abrasion (Mattinson, 2005) before dissolution, chemical separation (for grains >1 µg), and measurement following the technique of Krogh (1973). Detailed analytical procedures for the Oslo laboratory are given in Corfu (2004). Titanite was dissolved on a hotplate and processed with a single stage HCl-HBr procedure. Blanks are <2 pg for Pb and 0.1 pg for U. The initial Pb in titanite was corrected using a composition calculated with the Stacey and Kramers (1975) model at 0.5 Ga. Decay constants are from Jaffey et al. (1971). The plotting was done with the Isoplot program (Ludwig, 2009).

Selection of zircon grains targeted the youngest growth phase detectable in the population such as tips or visible overgrowths. The populations of the two anatectic granites (samples 4 and 113) are dominated by generally subhedral grains, locally with still preserved euhedral shapes, but mostly somewhat subhedral to anhedral (File DR4). Three zircon tips were analyzed for each of the samples (Table 1). The analyses are between 4% and 40% discordant (Fig. 2), and approximate a line with an upper intercept at ca. 2.46 Ga (mean square weighted deviation [MSWD] = 29). Two grains of the abundant U-rich (300 ppm) titanite, however, plot close to the lower intercept of the zircon discordia line (i.e., at ca. 0.5 Ga).

The foliated granite sample 96 contains similar zircon as the migmatites, with locally visible cores and overgrowths. The selection of tips and some prisms turned into very brittle fragments after chemical abrasion and the three analyses are between 6 and 15% discordant. These again approximate a line (MSWD = 7.1) and yield an upper intercept age of 2.387 ± 0.045 Ma (Fig. 2).

The other non-anatectic foliated granite sample (9) exhibits a variety of morphologies including prismatic subhedral to euhedral grains, but also anhedral grains and prisms with clearly visible cores and overgrowths (File DR4). Some of these overgrowths were mechanically separated from the cores, and two of them were analyzed. Other analyses were done of two tips and two fragments of long prismatic grains (File DR4). These four analyses are discordant and plot close to a line (MSWD = 129) with an upper intercept at ca. 2.45 Ga (Fig. 2). The two separated overgrowths, however, plot distinctly to the left of the discordia indicating growth or (and) isotopic disturbances during younger Proterozoic events. A line projected through the youngest data point from the titanite (at 0.5 Ga, see below) intersect the concordia curve at 2.23 Ga (Fig. 2), but it is not possible to know how reliable this intercept age is because of the nature of the discordia. The four titanite analyses together define a line with a lower intercept age of 0.502 ± 0.003 Ga, and an upper intercept at around 2.4 Ga, though imprecise due to the long extrapolation.

DISCUSSION

The results obtained from the zircon populations indicate growth at ca. 2.45–2.46 Ga in the migmatites (sample 4 and 113), and somewhat later in granite (96). The granite (9) has a main population suggesting the same age as the migmatites, but also younger overgrowths reflecting later growth or disturbances. The general morphological and isotopic features of the zircon data are consistent with a period of granite emplacement at around 2.45 Ga, similar to those recorded elsewhere in the Bastar Craton (cf. Mohanty, 2015; Bhattacharya et al., 2016; Chatterjee et al., 2017).

Several aspects of the U–Pb data need to be discussed for understanding the evolution of the Ranmal migmatites and foliated granites. The first notable aspect is the large degree of discordance in zircon ages, in spite of the generally good quality of the analyzed grains (Fig. 2), and the use of chemical abrasion (CA), which effectively reduces the effects of secondary Pb loss. The second important issue is the near-concordant titanite age at near 0.5 Ga. It is unclear whether the small discordance in titanite ages reflects old cores, incomplete resetting of old titanite, or incorrect common Pb correction. The fact that analyses of separate grains are identical for each sample suggests interferences due to the presence of older cores may not be a factor (rather it would be a coincidence), and this would also argue against resetting, although similar features have been seen, for example, in the Western Gneiss Complex (Tucker et al., 1987). The exact reason notwithstanding, the age of the titanite implies growth or a very strong overprint at 0.5 Ga, a view that is reinforced by the high U content and high Th/U values. Based on these data, the most likely conclusion is that the granites are Paleoproterozoic emplacements, but they were reactivated and partially re-melted during tectonic events at 0.502 ± 0.003 Ga.

TABLE 1. U-Pb DATA OF ZIRCON FROM RANMAL MIGMATITIC COMPLEX, BASTAR CRATON, EASTERN GHATS PROVINCE, INDIA

Characteristics[1]	Weight (μg)[2]	U (ppm)[2]	Th/U[3]	Pbi[4] (ppm)	Pbc[5] (pg)	$^{206}Pb/^{204}Pb$[6]	$^{207}Pb/^{235}U$[7]	2σ (abs)	$^{206}Pb/^{238}U$[7]	2σ (abs)	rho	$^{206}Pb/^{238}U$[7] (Ma)	$^{207}Pb/^{235}U$[7] (Ma)	$^{207}Pb/^{206}Pb$[7] (Ma)	2σ (abs)	D[8] (%)
Sample 4: anatectic granite, medium grained																
Z TIP CA [1]	20	367	0.71	0.0	1.4	145247	9.764	0.025	0.44351	0.00102	0.97	2366	2413	2452.2	1.2	4.2
Z TIP CA [1]	11	318	0.72	0.0	2.6	36394	9.569	0.025	0.43688	0.00099	0.96	2337	2394	2443.6	1.2	5.2
Z LONG TIP CA [1]	2	831	0.78	3.0	8.8	4840	8.846	0.021	0.40853	0.00084	0.95	2208	2322	2424.1	1.2	10.5
Sample 113: anatectic granite, medium grained																
Z TIP CA [1]	8	325	0.61	0.0	1.4	50560	9.242	0.024	0.42363	0.00098	0.96	2277	2362	2436.8	1.3	7.8
Z TIP CA [1]	2	429	0.63	1.4	5.1	4316	8.843	0.024	0.40944	0.00092	0.94	2212	2322	2419.7	1.6	10.1
Z TIP CA [1]	7	302	0.84	0.3	4.3	7666	4.777	0.014	0.24830	0.00060	0.95	1430	1781	2221.5	1.6	39.7
TIT B-RD FR NA [1]	173	305	2.07	2.1	360	766	0.655	0.005	0.08149	0.00044	0.78	505	512	541	10	6.8
TIT B-RFR NA [1]	91	319	1.97	2.2	203	749	0.654	0.004	0.08163	0.00033	0.71	506	511	533	10	5.3
Sample 9: foliated granite, medium grained																
Z TIP CA [1]	6	251	0.82	0.0	0.9	40873	8.625	0.022	0.39948	0.00088	0.96	2167	2299	2419.3	1.3	12.3
Z LP-FR CA [1]	1	304	0.95	0.0	0.5	14152	7.806	0.024	0.37284	0.00095	0.92	2043	2209	2366.9	2.1	16.0
Z LP-FR CA [1]	10	137	0.75	0.0	1.5	20387	7.665	0.021	0.36650	0.00088	0.95	2013	2193	2365.1	1.5	17.3
Z TIP CL CA [1]	10	154	0.82	0.0	1.2	28340	7.439	0.020	0.35482	0.00084	0.96	1958	2166	2369.3	1.4	20.1
Z PIECE OF TIP BR-O-C CA [1]	1	360	0.24	0.0	0.5	14910	7.002	0.020	0.35531	0.00089	0.94	1960	2112	2263.1	1.8	15.5
Z TIP-BR-O-C CA [1]	1	1204	0.23	0.0	0.5	49175	6.589	0.020	0.34956	0.00095	0.96	1932	2058	2185.9	1.5	13.4
TIT B-R FR NA [1]	18	167	4.55	1.9	36.4	446	0.680	0.005	0.08267	0.00024	0.44	512	527	593	15	14.2
TIT B-R FR NA [2]	22	210	5.07	2.2	51.6	481	0.682	0.006	0.08272	0.00028	0.51	512	528	597	16	14.7
Sample 96: weakly foliated granite, fine-grained																
Z TIP CA BRITTLE [10]	9	231	0.30	0.0	1.0	57270	8.817	0.024	0.41742	0.00103	0.97	2249	2319	2381.8	1.2	6.6
Z TIP CA BRITTLE [4]	1	259	0.57	0.0	0.5	12911	8.411	0.028	0.39976	0.00118	0.93	2168	2276	2375.3	2.1	10.3
Z TIP CA [1]	1	765	0.60	0.0	0.5	40652	8.111	0.046	0.38546	0.00213	0.99	2102	2243	2375.3	1.5	13.5

[1]Z—zircon; T—titanite; LP-FR—pieces of long prisms; BR-O-C—overgrowth broken away from cores; B-R—brown-red; CA—chemical abrasion; NA—no abrasion: [1] = number of grains in fraction.
[2,4]Weight and concentrations are known to be better than 10%, except for those near and below the ~1 μg limit of resolution of the balance.
[3]Th/U model ratio inferred from 208/206 ratio and age of sample.
[4]Pbi—initial common Pb.
[5]Pbc—total common Pb in sample (initial +blank).
[6]Raw data corrected for fractionation and blank.
[7]Corrected for fractionation, spike, blank and initial common Pb; error calculated by propagating the main sources of uncertainty.
[8]D—degree of discordancy.

The lack of concordant Cambrian zircon grains is a point for concern. The Zr contents in the Ranmal migmatites and non-migmatic, yet deformed granites (this study; Bhadra et al., 2007) plot below the Zr saturation curves at 750 °C and 850 °C (File DR5). This implies that new crystallization of zircons at 0.502 ± 0.003 Ga, especially in the high-T leucosomes was impeded due to Zr under-saturation at the temperature (~750 °C) of melting in the Ranmal migmatites.

In this context, the U–Pb zircon SHRIMP ages (Chatterjee et al., 2017) obtained in migmatitic quartzofeldspathic gneiss from the Bastar Craton and Eastern Ghats granulites in the Dharamgarh-Deobhog area (located ~50 km NW of Ranmal) across the EGB–Craton tectonic contact (Gupta et al., 2000) are instructive. As in this study, the cratonic gneiss in the area yielded discordant U–Pb isotope ratios that were resolved into 2.425 ± 0.032 Ga and 0.545 ± 0.034 Ga upper and lower intercept ages respectively (Chatterjee et al., 2017). By contrast, the EGP granulites yielded single-population concordant ^{238}U–^{206}Pb zircon ages between 0.534 ± 0.029 Ga and 0.510 ± 0.024 Ga, with no evidence of early Neoproterozoic dates that characterize the EGP (Chatterjee et al., 2017).

The 2.5–2.4 Ga upper intercept ages in the Bastar Craton granites (Fig. 2) are similar to the Late Neoarchean/Early Paleoproterozoic emplacement ages reported for granites elsewhere in the Bastar Craton (summary in Mohanty, 2015; Bhattacharya et al., 2016). The ca. 0.5 Ga lower intercept ages in zircon and the 0.502 Ga age of titanite in leucosomes in the anatectic migmatites document the first report of Pan African crustal anatexis experienced by the Bastar Craton synchronous with the top-to-the-west thrusting of the Neoproterozoic EGP (Fig. 3). The noteworthy feature of the age determinations in this study and those of Chatterjee et al. (2017) is the lack of 1.0–0.9 Ga ages in the Bastar Craton. By implication, the EGP did not juxtapose with the cratonic nucleus of the Greater India landmass, of which the Bastar Craton is an integral part, at least in the Early Neoproterozoic (Dalziel, 1997; Black et al., 1987; Mezger and Cosca, 1999; Dobmeier and Raith, 2003; Halpin et al., 2005; Chattopadhyay et al., 2015).

In the Rayner Complex, several authors provide compelling evidence for Pan African high-T metamorphism strongly overprinting the Grenvillian-age granulites (Harley and Buick, 1992; Hensen and Zhou, 1995; Fitzsimons et al., 1997; Phillips et al., 2009; Morrissey et al., 2016). By contrast, no demonstrable evidence has been put forth in favor of widespread high-T Pan African overprinting in the EGP, barring its western and northern margins. In few studies based on chemographic and P–T pseudosection analyses, the near-isothermal decompression and retrograde segment of the reconstructed P–T path in the Grenvillian-age EGP granulites is tacitly ascribed to Pan African decompression (Das et al., 2008). But unequivocal structural and textural evidence for Pan African decompression-induced metamorphism—such as syn-tectonic mineral growth or juvenile magma emplacements along ductile shear zones in tensional or contractional setting (Block and Royden, 1990; Teyssier et al., 2005)—in support of the assumption are lacking. Toward this end, this

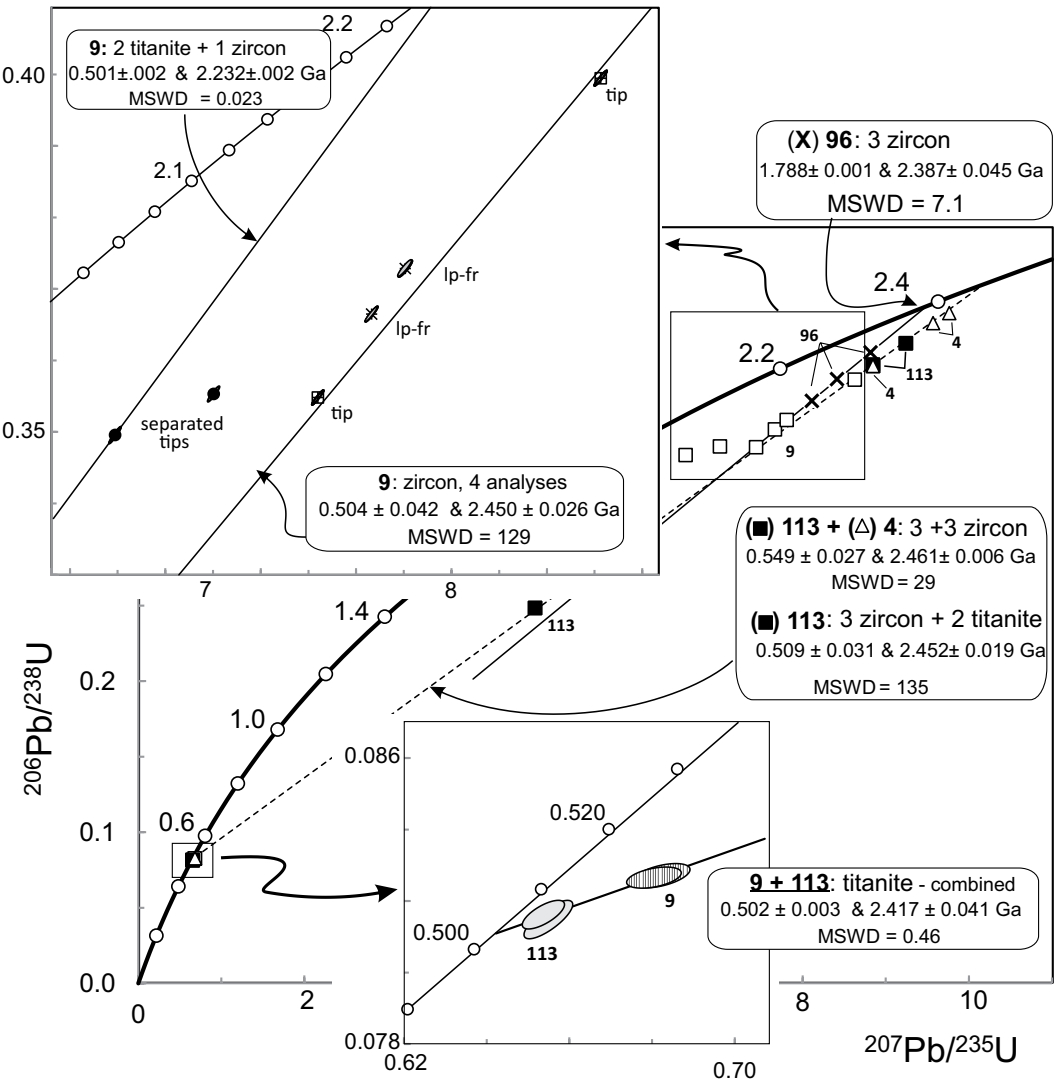

Figure 2. Concordia diagrams showing the U–Pb results for zircon and titanite in the four samples (locations in Fig. 1C). The ellipses indicate ± 2σ uncertainty, which is much smaller than the symbols used in the main plot. MSWD–mean square weighted deviation.

study provides the first geochronological evidence of high-T Pan African metamorphism leading to anatexis in the cratonic rocks fringing the EGP.

Integrating the aforementioned arguments with the paleogeographic reconstructions leads to the following scenarios. First, the Greater India landmass (excluding the EGP) accreted with the composite 1.0–0.9 Ga EGP–Rayner Complex as late as ca. 0.5 Ga (model A; Fig. 3) coinciding with the final assembly of the landmasses south of the equator into Gondwanaland, and not during the Early Neoproterozoic as has been suggested by some workers (Dobmeier and Raith, 2003; Chattopadhyay et al., 2015). Alternatively the EGP may have been detached from the composite EGP–Rayner Complex during the Rodinia break up at 0.75 Ga and was subsequently accreted to the Greater India landmass at ca. 0.5 Ga (model B; Fig. 3) as the landmass migrated from its position at northern latitudes it held at ca. 0.75 Ga (Fig. 1A). In the second model, the 0.5 Ga accretion of the EGP with the Bastar Craton vis-à-vis the Greater India landmass does not represent Indo-Antarctica accretion (model B; Fig. 3) in spite of the proximity suggested in the paleogeographic studies (Fig. 1A).

In the last decade and a half, several studies have highlighted the existence of Mid-Neoproterozoic ages (0.8–0.7 Ga) along the northern and western margins of the EGP, e.g. in the Chilka Lake anorthosite complex (Bose et al., 2016), along the Mahanadi shear zone (Veevers and Saeed, 2009; Bhattacharya et al., 2016), and in the Koraput syenite-anorthosite complex (Hippe et al., 2016; Saikia et al., 2018). Bose et al. (2016) suggest the age corresponds to high-grade metamorphism related to extensional tectonism in the EGP. This high-T extensional tectonic event is, however, not recorded in the Archean cratonic blocks neighboring the EGP (Biswal et al., 2007; Bhattacharya et al., 2016). This absence of Mid-Neoproterozoic ages in the cratonic nucleus in Eastern India provides tacit support to the proposition that the EGP–Bastar Craton accretion occurred at ca. 0.5 Ga, and not during the 1.0–0.9 Ga events. Moreover, the 0.8–0.7 Ga extensional tectonism maybe a vestige of the breakup of the EGP–Rayner Complex composite suggested in the model B in Figure 3.

CONCLUSIONS

Thrusting of the Grenvillian-age (1.0–0.9 Ga) granulites of the EGP over the Bastar Craton induced polyphase anatexis and deformation in granites of the cratonic footwall. U–Pb ages in the suite of anatectic migmatites, traceable to un-deformed granites in the hinterland, indicate

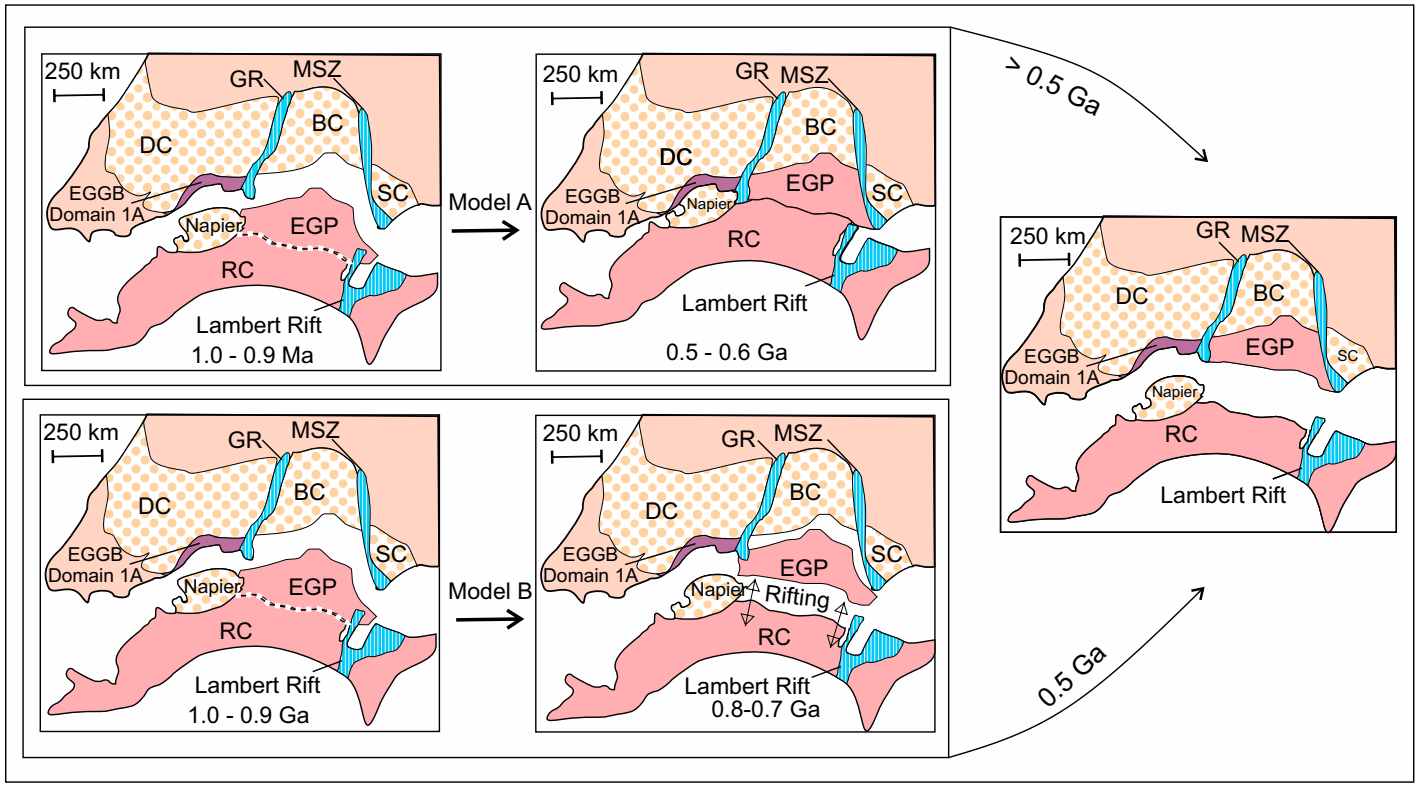

Figure 3. The top set figures (Model A) shows the composite 1.0–0.9 Ga EGP–Rayner Complex (RC) accreting with the Greater India landmass at 0.5 Ga. The bottom set figures (Model B) shows the 1.0–0.9 Ga EGP dismembered from the RC and Antarctica at 0.75 Ga before being accreted with the Greater India landmass at 0.5 Ga. Model B implies that India did not accrete with Antarctica during the Gondwanaland assembly. Other abbreviations: BC—Bastar Craton; DC—Dharwar Craton; EGGB—Eastern Ghats Granulite Belt; EGP—Eastern Ghats Province; GR—Godavari Rift; MSZ—Mahanadi Shear Zone; SC—Singhbum Craton.

that anatexis (750–780 °C; 8–9 kbar) in the 2.5–2.4 Ga cratonic granites at the EGP– Bastar Craton interface occurred at ca. 0.5 Ga. The lack of 1.0–0.9 Ga ages in the cratonic granites/gneisses suggest the EGP did not accrete with the Bastar Craton vis-à-vis the Greater India landmass in the Early Neoproterozoic. We suggest that the EGP—presumably coherently evolved with the Rayner Complex (Antarctica) at 1.0–0.9 Ga—welded with India at ca. 0.5 Ga culminating with the final assembly of the East Gondwanaland. Alternately the EGP may have dismembered from the EGP–Rayner Complex composite during the Rodinia break up and accreted with the Greater India landmass in the Cambrian. Therefore, India and Antarctica may not have accreted until late in the Cambrian, in spite of the close positioning of the two landmasses at 1.0–0.9 Ga and 0.6–0.5 Ga, inferred from paleogeographic considerations.

ACKNOWLEDGMENTS

Dicton Saikia is acknowledged for his help during field work. PN acknowledges financial support from Science and Engineering Research Board, Government of India through research project no. EMR/2014/000538. Dr. A.K. Singh, Wadia Institute of Himalayan Geology, and Dr. M. Satyanarayanan, National Geophysical Research Institute, are acknowledged for the geochemical analysis. We thank Tamer Abu-Alam and Kurt Stüwe for their comments that helped to improve the scientific rigor of the manuscript.

REFERENCES CITED

Bhadra, S., and Bhattacharya, A., 2007, The barometer tremolite + tschermakite + 2 albite = 2 pargasite + 8 quartz: Constraints from experimental data at unit silica activity, with application to garnet-free natural assemblages: The American Mineralogist, v. 92, p. 491–502, https://doi.org/10.2138/am.2007.2067.

Bhadra, S., Das, S., and Bhattacharya, A., 2007, Shear zone-hosted migmatites (eastern India): The role of dynamic melting in the generation of REE-depleted felsic melts, and implications for disequilibrium melting: Journal of Petrology, v. 48, p. 435–457, https://doi.org/10.1093/petrology/egl066.

Bhattacharya, A., Das, H.H., Bell, E., Bhattacharya, A., Chatterjee, N., Saha, L., and Dutt, A., 2016, Restoration of Late Neoarchean–Early Cambrian tectonics in the Rengali orogen and its environs (eastern India): The Antarctic connection: Lithos, v. 263, p. 190–212, https://doi.org/10.1016/j.lithos.2016.06.006.

Biswal, T.K., DeWaele, B., and Ahuja, H., 2007, Timing and dynamics of the juxtaposition of the Eastern Ghats Mobile Belt against the Bhandara craton, India: A structural and zircon U–Pb SHRIMP study of the fold-thrust belt and associated nepheline syenite plutons: Tectonics, v. 26, p. 1–21, https://doi.org/10.1029/2006TC002005.

Black, L.P., Harley, S.L., Sun, S.S., and McCulloch, M.T., 1987, The Rayner complex of East Antarctica: Complex isotopic systematics within a Proterozoic mobile belt: Journal of Metamorphic Geology, v. 5, p. 1–26, https://doi.org/10.1111/j.1525-1314.1987.tb00366.x.

Block, L., and Royden, L., 1990, Core complex geometries and regional scale flow in the lower crust: Tectonics, v. 9, p. 557–567, https://doi.org/10.1029/TC009i004p00557.

Bose, S., Dunkley, D., Dasgupta, S., Das, K., and Arima, M., 2011, India-Antarctica-Australia-Laurentia connection in the Paleoproterozoic–Mesoproterozoic revisited: Evidence from new zircon U-Pb and monazite chemical age data from the Eastern Ghats Belt, India: Geological Society of America Bulletin, v. 123, p. 2031–2049, https://doi.org/10.1130/B30336.1.

Bose, S., Das, K., Torimoto, J., Arima, M., and Dunkley, D.J., 2016, Evolution of the Chilka Lake granulite complex, northern Eastern Ghats Belt, India: First evidence of ~ 780 Ma decompression of the deep crust and its implication on the India–Antarctica correlation: Lithos, v. 263, p. 161–189, https://doi.org/10.1016/j.lithos.2016.01.017.

Chakraborty, P.P., Saha, S., and Das, R., 2015, Geology of Mesoproterozoic Chhattisgarh Basin, central India: Current status and future goals: Geological Society, London, Memoirs, v. 43, p. 185–205.

Chatterjee, A., Das, K., Bose, S., and Hidaka, H., 2017, Age-integrated tectonic evolution across the orogen-craton boundary: Age zonation and shallow- to deep crustal participation during Late Cambrian cratonisation of Eastern Ghats Belts, India: Lithos, v. 290–291, p. 269–293, https://doi.org/10.1016/j.lithos.2017.07.020.

Chattopadhyay, S., Upadhyay, D., Nanda, J.K., Mezger, K., Pruseth, K.L., and Berndt, J., 2015, Proto-India was a part of Rodinia: Evidence from Grenville-age suturing of the eastern Ghats Province with the Paleoarchean Singhbhum craton: Precambrian Research, v. 266, p. 506–529, https://doi.org/10.1016/j.precamres.2015.05.030.

Corfu, F., 2004, U-Pb age, setting, and tectonic significance of the anorthosite-mangerite-charnockite-granite-suite, Lofoten-Vesterålen, Norway: Journal of Petrology, v. 45, p. 1799–1819, https://doi.org/10.1093/petrology/egh034.

Dalziel, I.W.D., 1997, Neoproterozoic–Paleozoic geography and tectonics: Review, hypothesis and environmental speculation: Geological Society of America Bulletin, v. 109, p. 16–42, https://doi.org/10.1130/0016-7606(1997)109<0016:ONPGAT>2.3.CO;2.

Das, K., Yokoyama, K., Chakraborty, P.P., and Sarkar, A., 2009, Basal tuffs and contemporaneity of the Chattisgarh and Khariar basins based on new dates and geochemistry: The Journal of Geology, v. 117, p. 88–102, https://doi.org/10.1086/593323.

Das, S., Nasipuri, P., Bhattacharya, A., and Swaminathan, S., 2008, The thrust-contact between the Eastern Ghats Belt and the adjoining Bastar craton (Eastern India): Evidence from mafic granulites and tectonic implications: Precambrian Research, v. 162, p. 70–85, https://doi.org/10.1016/j.precamres.2007.07.013.

Dobmeier, C., and Raith, M.M., 2003, Crustal architecture and evolution of the Eastern Ghats Belt and adjacent regions of India, *in* Yoshida, M., Windley, B.E., and Dasgupta, S., eds., Proterozoic East Gondwana: Supercontinent Assembly and Breakup: Geological Society, London Special Publication 206, p. 145–168, https://doi.org/10.1144/GSL.SP.2003.206.01.09.

Fitzsimons, I.C.W., Kinny, P.D., and Harley, S.L., 1997, Two stages of zircon and monazite growth in anatectic leucogneiss: SHRIMP constraints on the duration and intensity of Pan-African metamorphism in Prydz Bay, East Antarctica: Terra Nova, v. 9, p. 47–51, https://doi.org/10.1046/j.1365-3121.1997.d01-8.x.

Gervasoni, F., Klemme, S., Eduardo Rocha-Júnior, R.V., and Berndt, J., 2016, Zircon saturation in silicate melts: A new and improved model for aluminous and alkaline melts: Contributions to Mineralogy and Petrology, v. 171, p. 1–12, https://doi.org/10.1007/s00410-016-1227-y.

Gupta, S., Bhattacharya, A., Raith, M., and Nanda, J.K., 2000, Pressure-temperature deformation history across a vestigial craton-mobile belt boundary: The western margin of Eastern Ghats Belt at Deobhog, India: Journal of Metamorphic Geology, v. 18, p. 683–697.

Halpin, J.A., Gerakiteys, C.L., Clarke, G.L., Belousova, E.A., and Griffin, W.L., 2005, In-situ U–Pb geochronology and Hf isotope analyses of the Rayner complex, East Antarctica: Contributions to Mineralogy and Petrology, v. 148, p. 689–706, https://doi.org/10.1007/s00410-004-0627-6.

Harley, S.L., and Buick, I.S., 1992, Wollastonite-scapolite assemblages as indicators of granulite pressure–temperature-fluid histories: The Rauer group, East Antarctica: Journal of Petrology, v. 33, p. 693–728, https://doi.org/10.1093/petrology/33.3.693.

Hensen, B.J., and Zhou, B., 1995, A pan-African granulite facies metamorphic episode in Prydz Bay, Antarctica: Evidence from Sm–Nd garnet dating: Australian Journal of Earth Sciences, v. 42, p. 249–258, https://doi.org/10.1080/08120099508728199.

Hippe, K., Moller, A., Quadt, von A., Peytcheva, I., and Hammerschmidt, K., 2016, Zircon geochronology of the Koraput alkaline Complex: Insights from combined geochemical and U-Pb-Hf isotopic analyses and implications for the timing of alkaline magmatism in the Eastern Ghats Belt, India: Gondwana Research, v. 34, p. 205–220, https://doi.org/10.1016/j.gr.2015.02.021.

Holland, T.J.B., and Blundy, J., 1994, Non-ideal interactions in calcic amphiboles and their bearing on amphibole-plagioclase thermometry: Contributions to Mineralogy and Petrology, v. 116, p. 433–447, https://doi.org/10.1007/BF00310910.

Jaffey, A.H., Flynn, K.F., Glendenin, L.E., Bentley, W.C., and Essling, A.M., 1971, Precision measurement of half-lives and specific activities of ^{235}U and ^{238}U: Physical Review, v. 4, p. 1889–1906.

Krogh, T.E., 1973, A low contamination method for hydrothermal decomposition of zircon and extraction of U and Pb for isotopic age determinations: Geochimica et Cosmochimica Acta, v. 37, p. 485–494, https://doi.org/10.1016/0016-7037(73)90213-5.

Li, Z.X., Bogdanova, S.V., Collins, A.S., Davidson, A., De Waele, B., Ernst, R., Evans, D., Fitzsimons, I.C.W., Fuck, R.A., Gladkochub, D.P., Jacobs, J., Karlstrom, K.E., Lu, S., Natapov, L., Pease, V., Pisarevsky, S.A., Thrane, K., and Vernikovsky, V., 2008, Assembly, configuration, and break-up history of Rodinia: A synthesis: Precambrian Research, v. 160, p. 179–210, https://doi.org/10.1016/j.precamres.2007.04.021.

Ludwig, K.R., 2009, Isoplot 4.1. A geochronological toolkit for Microsoft Excel: Berkeley Geochronology Centre Special Publications, v. 4, p. 76.

Mattinson, J.M., 2005, Zircon U-Pb chemical abrasion ("CA-TIMS") method: Combined annealing and multi-step partial dissolution analysis for improved precision and accuracy of zircon ages: Chemical Geology, v. 220, p. 47–66, https://doi.org/10.1016/j.chemgeo.2005.03.011.

Mezger, K., and Cosca, M., 1999, The thermal history of the eastern Ghats Belt (India), as revealed by U–Pb and ^{40}Ar/^{39}Ar dating of metamorphic and magmatic minerals: Implications for the SWEAT hypothesis: Precambrian Research, v. 94, p. 251–271, https://doi.org/10.1016/S0301-9268(98)00118-1.

Mohanty, S.P., 2015, Palaeoproterozoic supracrustals of the Bastar Craton: Dongargarh supergroup and Sausar group, *in* Mazumder, R., Eriksson, P.G., eds., Precambrian Basins of India: Stratigraphic and Tectonic Context: Geological Society, London, Memoirs, v. 43, p. 151–164, https://doi.org/10.1144/M43.11.

Morrissey, L.J., Hand, M., and Kelsey, D.E., 2015, Multi-stage metamorphism in the Rayner–Eastern Ghats Terrane: P–T–t constraints from the northern Prince Charles Mountains, East Antarctica: Precambrian Research, v. 267, p. 137–163, https://doi.org/10.1016/j.precamres.2015.06.003.

Morrissey, L.J., Hand, M., Kelsey, D.E., and Wade, B.P., 2016, Cambrian High-temperature Reworking of the Rayner–Eastern Ghats Terrane: Constraints from the Northern Prince Charles Mountains Region, East Antarctica: Journal of Petrology, v. 57, p. 53–92, https://doi.org/10.1093/petrology/egv082.

Phillips, G., Kelsey, D.E., Corvino, A.F., and Dutch, R.A., 2009, Continental reworking during overprinting orogenic events, southern Prince Charles Mountains, East Antarctica: Journal of Petrology, v. 50, p. 2017–2041, https://doi.org/10.1093/petrology/egp065.

Rickers, K., Mezger, K., and Raith, M.M., 2001, Evolution of the continental crust in the Proterozoic eastern Ghats Belt, India and new constraints for Rodinia reconstruction: Implications from Sm–Nd, Rb–Sr and Pb–Pb isotopes: Precambrian Research, v. 112, p. 183–212, https://doi.org/10.1016/S0301-9268(01)00146-2.

Saikia, D., Nasipuri, P., and Bhattacharya, A., 2018, In situ U–Th–Pb $_{total}$ dating of polychronous monazite in the Koraput anorthosite pluton, Eastern Ghats Granulite Belt (India), and implications: Geological Magazine, v. 155, p. 209–228, https://doi.org/10.1017/S001675681700084X.

Stacey, J.S., and Kramers, J.D., 1975, Approximation of terrestrial lead isotope evolution by a two-stage model: Earth and Planetary Science Letters, v. 26, p. 207–221, https://doi.org/10.1016/0012-821X(75)90088-6.

Torsvik, T.H., 2003, The Rodinia Jigsaw Puzzle: Science, v. 300, p. 1379–1381, https://doi.org/10.1126/science.1083469.

Tucker, R.D., Råheim, A., Krogh, T.E., and Corfu, F., 1987, Uranium-lead zircon and titanite ages from the northern portion of the Western Gneiss Region, south-central Norway: Earth and Planetary Science Letters, v. 81, p. 203–211, https://doi.org/10.1016/0012-821X(87)90156-7.

Teyssier, C., Ferré, E.C., Whitney, D.L., Norlander, B., Vanderhaeghe, O., and Parkinson, D., 2005, Flow of partially molten crust and origin of detachments during collapse of the Cordilleran Orogen, *in* Bruhn, D., and Burlini, L., eds., High Strain Zones: Structure and Physical Properties: Geological Society, London, Special Publications 245, p. 39–64, https://doi.org/10.1144/GSL.SP.2005.245.01.03.

Veevers, J.J., and Saeed, A., 2009, Permian–Jurassic Mahanadi and Pranhita–Godavari Rifts of Gondwana India: Provenance from regional paleoslope and U-Pb/Hf analysis of detrital zircons: Gondwana Research, v. 16, p. 633–654, https://doi.org/10.1016/j.gr.2009.05.013.

MANUSCRIPT RECEIVED 8 SEPTEMBER 2017
REVISED MANUSCRIPT RECEIVED 19 FEBRUARY 2018
MANUSCRIPT ACCEPTED 2 APRIL 2018